AN EVALUATION OF CHARPY ENERGY VS TEMPERATURE CURVE - FITTING TECHNIQUES

W. H. Cullen, Jr., J. R. Hawthorne, and L. F. Garroway

ABSTRACT

Several sets of Charpy energy vs temperature data, spanning a range of typical characteristics, have been analyzed using different curve fitting techniques, and the results compared with the authors' estimates of certain critical parameters. The curve fitting functions, the hyperbolic tangent, a polynomial and a piecewise curvilinear form, yielded, for the most part, reasonably equivalent results. The authors' estimates were, in each case, more conservative, but not significantly different from the computer-generated results. Some of the potential hazards of computer-generated curve-fitting analyses are indicated, including a problem in which some computer algorithms may converge on a non-optimum set of coefficients.

AN EVALUATION OF CHARPY ENERGY VS TEMPERATURE CURVE - FITTING TECHNIQUES

INTRODUCTION

There have been several attempts to determine, through curve-fitting procedures, an analytical expression for the basically sigmoidal shape of Charpy energy vs temperature trend for ferritic steels. Total and piece wise polynomial functions, expressions based in probability theory, expressions derived from nucleation and growth theory, and transcendental functions, such as hyperbolic tangents and various exponential-based functions, have all been tested with varying degrees of success. An adequate, curve-fitted expression, if one can be found, would be significant since, through its parameters, or coefficients, it would provide a standardized basis for material-to-material comparison, and would uniquely define the 41 and 68 joule level temperatures, upper and lower shelf energy values, and other parameters of interest to engineers who use this type of notch ductility data. Underlying all of the mathematical contortions is the basic question as to whether nature has endowed Charpy test results with any inherently sensible analytical form, or whether scientists must derive, not from first principles, but from imaginative creativity, a satisfactory function.

EXPERIMENTAL METHODS

A. Data Collection and Organization: Thirty-eight data sets were selected from the NRL archives and subjected to an evaluation using the various fitting procedures described later. These particular data sets were selected because they spanned a wide variety of materials, material conditions and data trend characteristics. Of these 38 sets, only the most significant sets of results (a total of eleven) are presented here. These selected examples represent curve-fits with varying degrees of success, from very good to meaningless, which demonstrate the effects of both poorly-and well-conditioned data, and the implications that poor data conditioning may have on the final results.

All of the Charpy data have been published earlier in the context of the response of these materials to irradiation. References 1-4 contain the basic data, the hand-drawn curves, and tabulations of the graphically interpolated results. In addition to this manual evaluation of the data, three different curve-fitting methods have been applied to some or all of the 38 data sets. All 38 sets were fitted with the hyperbolic tangent function (5,6) both with, and without an additional "fictitious" data point which served to help define a lower shelf energy level in those cases for which the data by itself did not adequately define this level. Twenty of the data sets (AEC-CE-NRL Cooperative Program results, Ref.(1) were also distributed to C. G. Interrante, of the National Bureau of Standards, who applied a polynomial fit to the data, and to Hofer and colleagues at Krafftwerk

Union, Erlangen, Germany, who applied the piecewise curvilinear fit described in Ref 7 and 8. Four sets of these twenty are included in the eleven sets presented in this report. The remaining eighteen data sets are found in Refs 2-4; seven of these are presented here as examples of curve-fitting results.

The data sets were evaluated by the cooperating scientists during the period 1978-early 1979. In the ensuing time interval, as may be expected in a rapidly developing technology, a number of changes have been suggested. Oldfield has offered a generalization of the hyperbolic tangent model which fits the rising lower and rising or falling upper shelf situations, at the expense of additional fitting parameters and the loss of physical identity of two of the four previously defined coefficients. Interrante has combined exponential and polynomial functions to form a piecewise curvilinear fit, much like the German method in its capability. All three methods are reasonably well-documented in a draft of a proposed method of test currently being circulated in ASTM Committee E-10.02.

B. Computational Methods: Conceptually, the hyperbolic tangent fitting procedure has been advanced by Oldfield (5,6). Oldfield has suggested a method of determining coefficients using a least differences technique, but in principle, least squares minimization techniques produce the same results. A program was written to determine the coefficients A, B, T_o and C in the formula

$$C_v = A + B \ \mathrm{Tanh}\left(\frac{T-T_o}{C}\right)$$

in which C_v is the Charpy energy measured at temperature T. The term T_o locates the point of inflection of the transition region while C is proportional to the "spread" of the transition. A + B and A-B represent the asymptotic values of the upper and lower shelf levels.

The computation of the coefficients was carried out on a large mainframe computer* using a standard least squares minimization routine, versions of which are readily available on most scientific subroutine packages. The computation of the initial guesses for each coefficient, the evaluation of the chosen function, and its derivatives with respect to its coefficients are performed by a user-written subprogram.

In this particular task, the computed results were stored on permanent disk files, and later passed to a small desktop computer system for plotting.** This technique saves the expense of computer-center-plotting, takes advantage of the high-resolution of modern desk-top plotters, and allows user-control of the plotting process.

---

* Texas Instruments Advanced Scientific Computer # 7.
**Hewlett-Packard System 9845A

PRESENTATION OF RESULTS:

The graphical results of the hyperbolic tangent fitting procedure are shown in Figs 1 to 11. The computed numerical values for upper and lower shelf energies, T_o, the temperature at the midpoint of the transition region, and the temperatures of the 41 and 68 J (30 and 50 ft-lb) levels are shown in Table 1a (SI units) and 1b (English units). Also shown in the tables are the graphically interpolated values of upper shelf energy and 41 and 68 J levels. For the four cases shown (Figs 1,3,6 and 8) for which the polynomial fit and the piecewise curvilinear results were available, the three temperature levels (T_o, 41 and 68 J temperatures) are also shown.

For each data set, the hyperbolic tangent curve was fitted under three conditions: (a) using just the experimental data, with each point weighted equally, and (b) and (c) adding a "fictitious" data point at -232 C, 7 J (-450 F, 5 ft-lb) with weights, relative to the experimental data, of 0.1 and 1.0. The purpose of this extra point is more for practical convenience than theoretical soundness. Without this extra point, or other such constraint, the resultant "best" fit of the hyperbolic tangent would generate, for some data sets, negative values of energy for the lower shelf level. In addition to being physically impossible, this is somewhat unpalatable to those examining these results who may not be familiar with this pitfall. Thus a significant effort has been made here to examine the effect and the necessity of adding this extra point.

Each figure also shows the coefficients A, B, T_o and C (in English units) determined for the best-fit conditions and the confidence limits ($\pm 2\,\sigma$ and $\pm 3\,\sigma$, σ = standard deviation) for the data in the transition region. This standard deviation was computed using only the data points in the transition region defined as $T_o - C \leq T \leq T_o + C$ using the T_o and C values of the resultant best fit. There are four degrees of freedom for this method, corresponding to the choice of the four coefficients, and so, for those data sets containing four, or fewer, data points in this transition region, no standard deviation could be computed.

While the figures themselves and Tables 1a and b speak rather completely of the conclusions of this study, the salient features of each figure are given below. The critical items to examine are: (a) the overall quality of the hyperbolic tangent fit, both with and without the extra point. (b) the effect of adding the extra point on the values of the important parameters. (c) the comparison of the results between the three computational methods, where available and (d) the comparison between the authors' estimates for the 41 and 68 J temperature levels, and the upper shelf energy level.

Fig. 1. This is a basically complete data set, spanning a temperature range complete enough to produce an easily distinguishable sigmoidal shape. There are only three data points in the transition region, so a standard deviation value could not be computed. Adding an extra data point results in little change of the significant parameters, the lower shelf value being the most affected. There is good agreement between the authors' estimates "based on hand-drawn curves" the polynomial fit and the hyperbolic tangent fits for the upper shelf and 68 J temperature value, with the piecewise curvilinear model giving values of about twenty centigrade degrees lower. There is somewhat less coordination among these values for the 41 J temperature level.

Table la - Results of Hyperbolic Tangent
Curve Fitting Techniques - Critical Values
(Metric Units)

Fig. 1 - Irradiated A533B

	(Joule)		(Degrees Centigrade)		
	Upper	Lower	To	41	68
a)	127	35	104	74	98
b)	127	35	104	74	97
c)	130	21	99	71	94
Interrante	—	—	82	84	94
Hofer, et al.	—	—	81	57	78
Ref. 1	126	—	—	60	99

Fig. 2 - Irradiated A533B

	Upper	Lower	To	41	68
a)	133	19	95	63	88
b)	134	18	94	63	88
c)	135	12	92	62	87
Ref. 2	133	—	—	63	91

Fig. 3 - Irradiated Weld Metal - A533B Parent Plate

	Upper	Lower	To	41	68
a)	213	1	10	-20	-6
b)	213	4	10	-20	-6
c)	213	6	11	-20	-6
Interrante	—	—	-2	—	-6
Hofer, et al.	—	—	3	-20*	-8*
Ref. 1	210	—	—	-15	-1

Fig. 4 - Irradiated A533B

	Upper	Lower	To	41	68
a)	260	-123	-43	-67	-44
b)	245	-6	5	-68	-38
c)	244	4	9	-73	-40
Ref. 3	217	—	—	-32	-21

Table la - Continued

Fig. 5 - Unirradiated A533B

	(Joule)		(Degrees Centigrade)		
	Upper	Lower	To	41	68
a)	147	-2	33	-1	28
b)	146	2	35	-1	28
c)	145	6	36	0	29
Ref. 3	137	—	—	-1	29

Fig. 6 - Irradiated Weld Metal - A533B Parent Plate

	Upper	Lower	To	41	68
a)	154	-26	55	26	59
b)	151	0	15	26	62
c)	150	6	74	26	62
Interrante	—	—	58	27	56
Hofer, et al.	—	—	66	26	58
Ref. 1	133	—	—	32	71

Fig. 7 - Irradiated A533B

	Upper	Lower	To	41	68
a)	243	-56	-6	-26	-15
b)	241	-23	1	-26	-14
c)	240	-2	5	-27	-14
Ref. 3	228	—	—	-23	-15

Fig. 8 - Irradiated Heat Affected Zone - A533B Parent Plate

	Upper	Lower	To	41	68
a)	636	-1088	-293	-14	16
b)	214	-11	58	-11	23
c)	209	3	63	-14	23
Interrante	—	—	56	—	25
Hofer, et al.	—	—	47	- 6*	23
Ref. 1	165	—	—	24	60

Table la - Continued

Fig. 9 - Irradiated A533B

	(Joule)		(Degrees Centigrade)		
	Upper	Lower	To	41	68
a)	165	1	47	6	34
b)	163	5	48	6	34
c)	163	6	49	4	33
Ref. 1	160	—	—	18	46

Fig. 10 - Irradiated Weld Metal - A508 Parent Plate

	Upper	Lower	To	41	68
a)	106	20	23	-14	29
b)	106	19	22	-13	29
c)	107	10	16	-14	29
Ref. 2	111	—	—	-12	29

Fig. 11 - Irradiated A302B

	Upper	Lower	To	41	68
a)	390	-2	64	-8	12
b)	331	0	55	-8	12
c)	257	3	42	-8	12
Ref. 4	118	—	—	-9	16

*Graphically extrapolated value

Table Ib - Results of Hyperbolic Tangent Curve Fitting Techniques - Critical Values (English Units)

Fig. 1 - Irradiated A533B

	(ft - lb)		(Degrees Fahrenheit)		
	Upper	Lower	To	30	50
a)	94	26	219	165	208
b)	94	25	219	166	207
c)	96	16	211	160	201
Interrante	—	—	179	183	202
Hofer, et al.	—	—	178	135	173
Ref. 1	93	—	—	140	210

Fig. 2 - Irradiated A533B

	Upper	Lower	To	30	50
a)	98	14	203	146	191
b)	99	13	202	146	191
c)	100	9	197	144	189
Ref. 2	98	—	—	145	195

Fig. 3 - Irradiated Weld Metal - A533B Parent Plate

	Upper	Lower	To	30	50
a)	157	1	50	-4	21
b)	157	3	51	-5	21
c)	157	5	52	-5	2
Interrante	—	—	28	—	22
Hofer, et al.	—	—	37	-4*	18*
Ref. 1	155	—	—	5	30

Fig. 4 - Irradiated A533B

	Upper	Lower	To	30	50
a)	192	-91	-45	-89	-47
b)	181	-4	41	-91	-37
c)	180	3	48	-90	-40
Ref. 3	160	—	—	-26	-6

Table Ib - Continued

Fig. 5 - Unirradiated A533B

	(ft -lb)		(Degrees Fahrenheit)		
	Upper	Lower	To	30	50
a)	109	-2	91	30	83
b)	108	2	95	31	83
c)	107	4	97	32	84
Ref. 3	101	—	—	30	84

Fig. 6 - Irradiated Weld Metal - A533B Parent Plate

	Upper	Lower	To	30	50
a)	114	-19	131	79	139
b)	111	0	59	78	143
c)	111	4	165	78	144
Interrante	—	—	137	81	132
Hofer, et al.	—	—	151	79	136
Ref. 1	98	—	--	90	160

Fig. 7 - Irradiated A533B

	Upper	Lower	To	30	50
a)	179	-42	22	-15	5
b)	178	-17	33	-15	6
c)	177	-1	41	-16	7
Ref. 3	168	—	—	-9	5

Fig. 8 - Irradiated Heat Affected Zone - A533B Parent Plate

	Upper	Lower	To	30	50
a)	469	-802	-496	6	61
b)	158	-8	136	13	73
c)	155	3	145	7	73
Interrante	—	—	132	—	77
Hofer, et al.	—	—	117	21*	73
Ref. 1	122	—	—	75	140

Table lb - Continued

Fig. 9 - Irradiated A533B

	(ft - lb)		(Degrees Fahrenheit)		
	Upper	Lower	To	30	50
a)	122	0.8	117	42	93
b)	120	4	119	42	93
c)	120	5	120	40	92
Ref. 1	118	—	—	65	115

Fig. 10 - Irradiated Weld Metal - A508 Parent Plate

	Upper	Lower	To	30	50
a)	78	15	73	7	85
b)	78	14	71	8	84
c)	79	8	60	6	84
Ref. 2	82	—	—	10	85

Fig. 11 - Irradiated A302B

	Upper	Lower	To	30	50
a)	288	-2	148	18	53
b)	244	-0	131	18	53
c)	189	2	107	19	53
Ref. 4	87	—	—	15	60

*Graphically extrapolated value

Fig. 1. Absorbed Charpy impact energy vs temperature for irradiated A533B steel, with hyperbolic tangent fits for three initial conditions: (a) no added low temperature point, (b) and (c) added point at -232 C, 7 J (-450 F, 5 ft-lb) with numerical weights of 0.1 and 1.0 respectively. For this wide spanned data set, there is little significant influence of the added data point. The lower shelf is the most affected of the significant values.

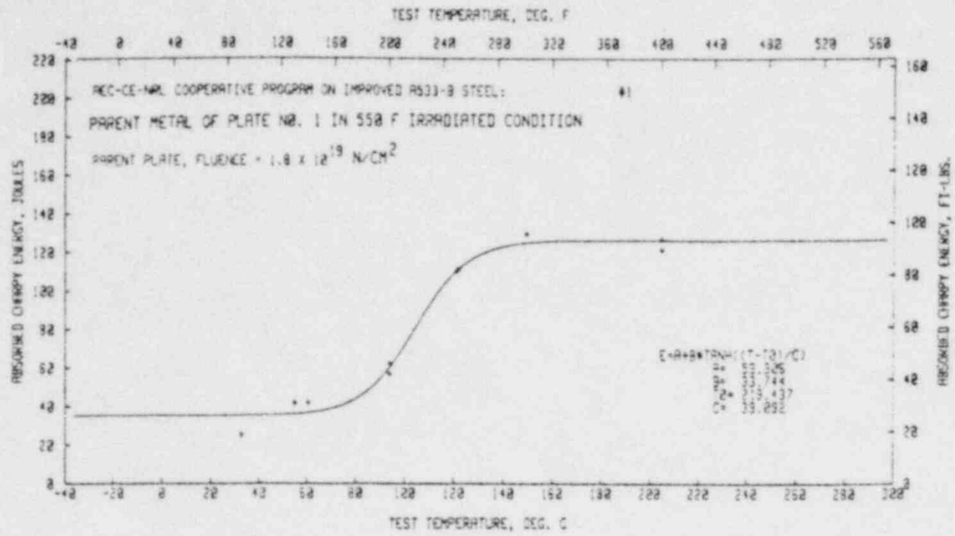
TEST TEMPERATURE, DEG. F
AEC-CE-NRL COOPERATIVE PROGRAM ON IMPROVED A533-B STEEL: #1
PARENT METAL OF PLATE NO. 1 IN 550 F IRRADIATED CONDITION
PARENT PLATE, FLUENCE = 1.8 X 10^19 N/CM^2
E=A+B*TANH((T-T0)/C)
ABSORBED CHARPY ENERGY, JOULES
ABSORBED CHARPY ENERGY, FT-LBS.
TEST TEMPERATURE, DEG. C

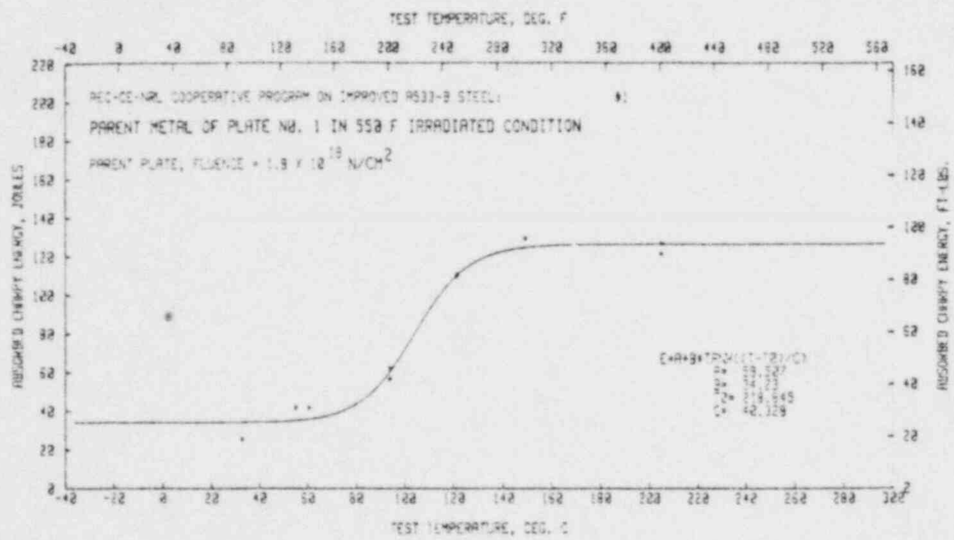
TEST TEMPERATURE, DEG. F
AEC-CE-NRL COOPERATIVE PROGRAM ON IMPROVED A533-B STEEL: #1
PARENT METAL OF PLATE NO. 1 IN 550 F IRRADIATED CONDITION
PARENT PLATE, FLUENCE = 1.8 X 10^19 N/CM^2
E=A+B*TANH((T-T0)/C)
ABSORBED CHARPY ENERGY, JOULES
ABSORBED CHARPY ENERGY, FT-LBS.
TEST TEMPERATURE, DEG. C

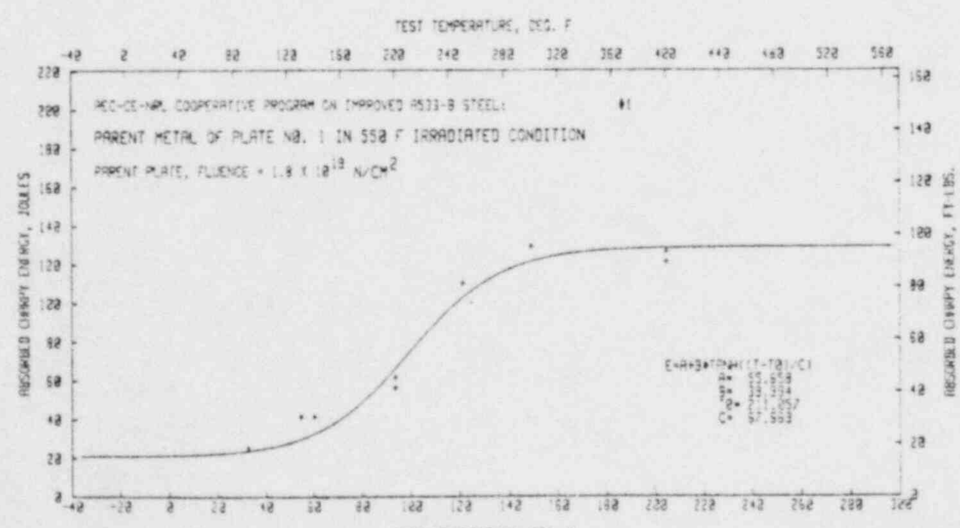
TEST TEMPERATURE, DEG. F
AEC-CE-NRL COOPERATIVE PROGRAM ON IMPROVED A533-B STEEL: #1
PARENT METAL OF PLATE NO. 1 IN 550 F IRRADIATED CONDITION
PARENT PLATE, FLUENCE = 1.8 X 10^19 N/CM^2
E=A+B*TANH((T-T0)/C)
ABSORBED CHARPY ENERGY, JOULES
ABSORBED CHARPY ENERGY, FT-LBS.
TEST TEMPERATURE, DEG. C

Fig. 2. As in Fig. 1, this is a well-spanned data set, addition of the extra point has little effect and the agreement among the computed model (tanh only) and the authors' estimates is excellent.

Fig. 3. Even though the lower shelf is not at all defined by the data, the upper shelf is, and the hyperbolic tangent fit succeeds in furnishing a positive value of the lower shelf energy even without the addition of the low temperature point. The agreement among the three computed models, and the authors' estimates is quite good.

Fig. 4. This is a very sparse data set and the lower shelf is quite undefined. It is, in fact, uncertain as to whether the upper shelf value is established, or whether the data continue to increase with temperature. With only five data points in the transition region, the standard deviation is quite large. Fitting the hyperbolic tangent without a fully weighted low temperature value results in negative values of the lower shelf energy. In spite of this, the computations of 41 and 68 joule temperatures is very consistent, but these values, and the upper shelf calculation all vary significantly from the author's estimates which were also based on a priori knowledge of the unirradiated condition data trend for the particular plate and the irradiation response of A533B.

Fig. 5. This is a reasonably well-distributed data set for which the hyperbolic tangent fit just barely fails to produce a positive lower shelf energy level in the absence of the extra point. Agreement between the computed results and the authors' estimates is excellent. (HSST PLATE 03)

Fig. 6. This data set is somewhat similar to that of Fig. 5, but with somewhat higher scatter and a larger violation of the positive lower shelf energy criteria. The agreement among the three computed models is very good, however the authors' estimates, again based in part, on a priori knowledge of the unirradiated condition properties of this material, are somewhat more conservatively figured.

Fig. 7. In this case, the hyperbolic tangent fit fails to produce a positive lower shelf value for the conditions tested here, although it is obvious that a slightly heavier weighting of the added point would have raised the lower shelf to a positive value. In spite of this minor shortcoming, the agreement between the computed results and the authors' estimate is excellent.

Fig. 8. This data set for weld heat affected zone (HAZ) material produced the most unrealistic values of any of the thirty-eight sets considered in this work. It is included among the final eleven not only because of this, rather academic, fact but also because all three of the computed models produced roughly the same results, which are significantly different from the authors' quite conservative, i.e. upper bound, estimates typically used for HAZ data. The authors' estimates were based, in part, on knowledge of the irradiation response of parent base plate material.

Fig. 9. This data set is included because it is an example of a "double shelf" material. It is not expected that the hyperbolic tangent model, with only four degrees of freedom, should accurately describe this behavior, and the final results represent an averaging phenomenon. Note, however, that the agreement in upper shelf values between authors and computer, is excellent, and that the 41 and 68 J levels differ by about ten Centigrade degrees, with the authors' values being the more conservative.

This page is left intentionally blank

Fig. 2. Absorbed Charpy impact energy vs temperature for irradiated A533B steel, with hyperbolic tangent fits for three initial conditions: (a) no added low temperature point, (b) and (c) added point at -232 C, 7 J (-450 F, 5 ft-lb) with numerical weights of 0.1 and 1.0 respectively. As in Fig. 1, the incorporation of an additional "fictitious" data point results in little significant adjustment of the important parameters of the fitting function.

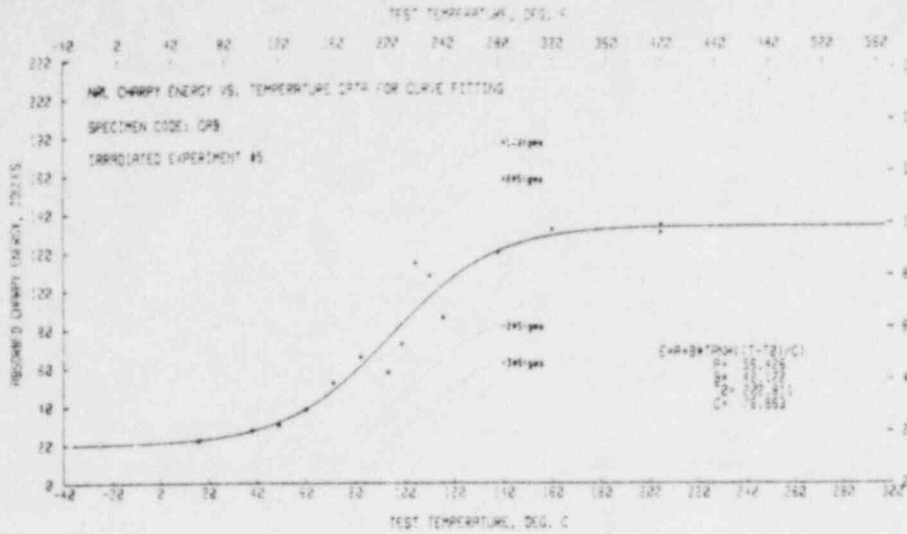
TEST TEMPERATURE, DEG. F
NRL CHARPY ENERGY VS. TEMPERATURE DATA FOR CURVE FITTING
SPECIMEN CODE: CP8
IRRADIATED EXPERIMENT #5
ABSORBED CHARPY ENERGY, JOULES
ABSORBED CHARPY ENERGY, FT-LBS.
TEST TEMPERATURE, DEG. C

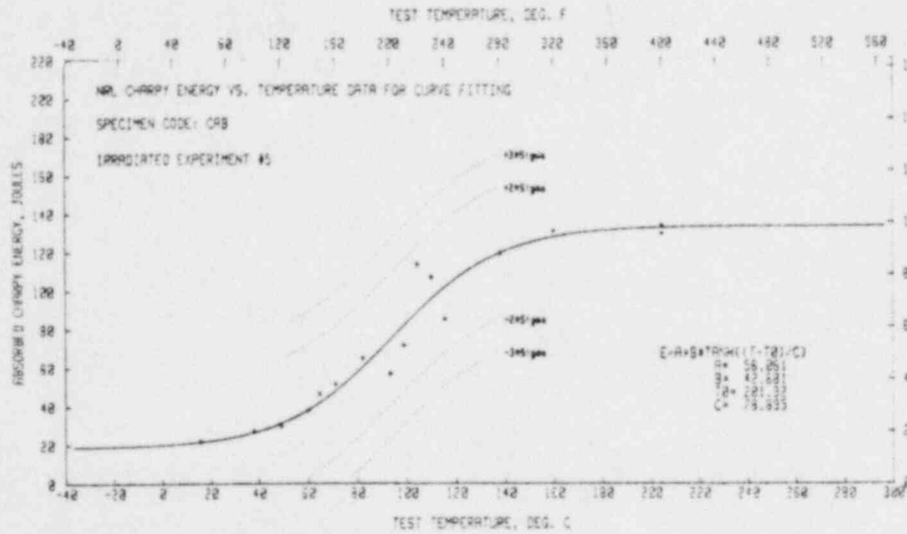
TEST TEMPERATURE, DEG. F
NRL CHARPY ENERGY VS. TEMPERATURE DATA FOR CURVE FITTING
SPECIMEN CODE: CP8
IRRADIATED EXPERIMENT #5
ABSORBED CHARPY ENERGY, JOULES
ABSORBED CHARPY ENERGY, FT-LBS.
E=A+B*TANH((T-T0)/C)
TEST TEMPERATURE, DEG. C

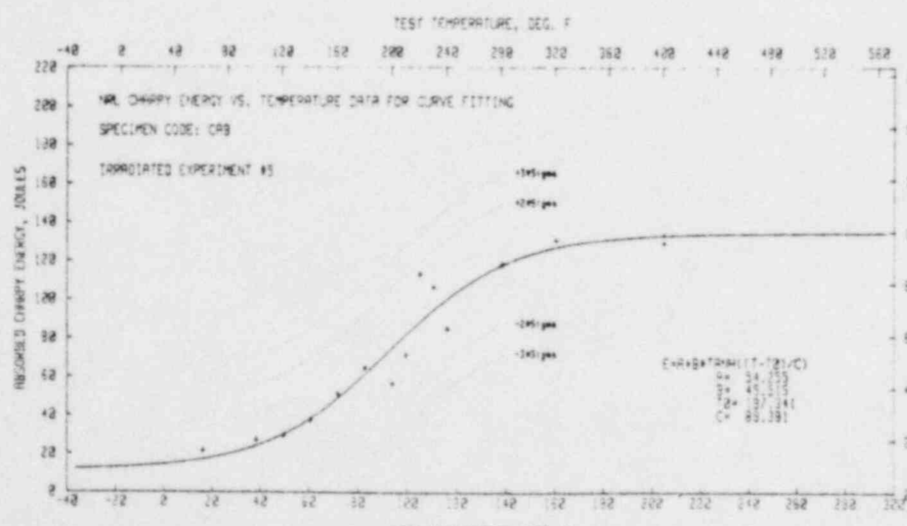
TEST TEMPERATURE, DEG. F
NRL CHARPY ENERGY VS. TEMPERATURE DATA FOR CURVE FITTING
SPECIMEN CODE: CP8
IRRADIATED EXPERIMENT #5
ABSORBED CHARPY ENERGY, JOULES
ABSORBED CHARPY ENERGY, FT-LBS.
E=A+B*TANH((T-T0)/C)
TEST TEMPERATURE, DEG. C

Fig. 3. Absorbed Charpy impact energy vs temperature for irradiated weld metal (A533B parent plate), with hyperbolic tangent fits for three initial conditions: (a) no added low temperature point, (b) and (c) added point at -232 C, 7 J (-450 F, 5 ft-lb) with numerical weights of 0.1 and 1.0 respectively. This data set is fit with just marginal success without the use of extra point.

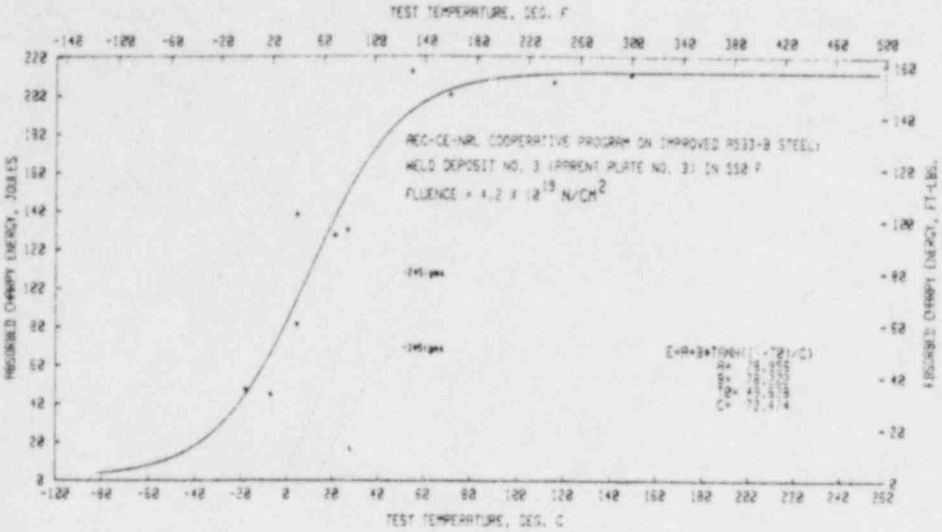
TEST TEMPERATURE, DEG. F
REC-CE-NRL COOPERATIVE PROGRAM ON IMPROVED A533-B STEEL:
WELD DEPOSIT NO. 3 (PARENT PLATE NO. 3) IN 550 F
FLUENCE = 4.2 X 10^19 N/CM^2
E=A+B*TANH((T-T0)/C)
C= 72.474
ABSORBED CHARPY ENERGY, JOULES
ABSORBED CHARPY ENERGY, FT-LBS.
TEST TEMPERATURE, DEG. C

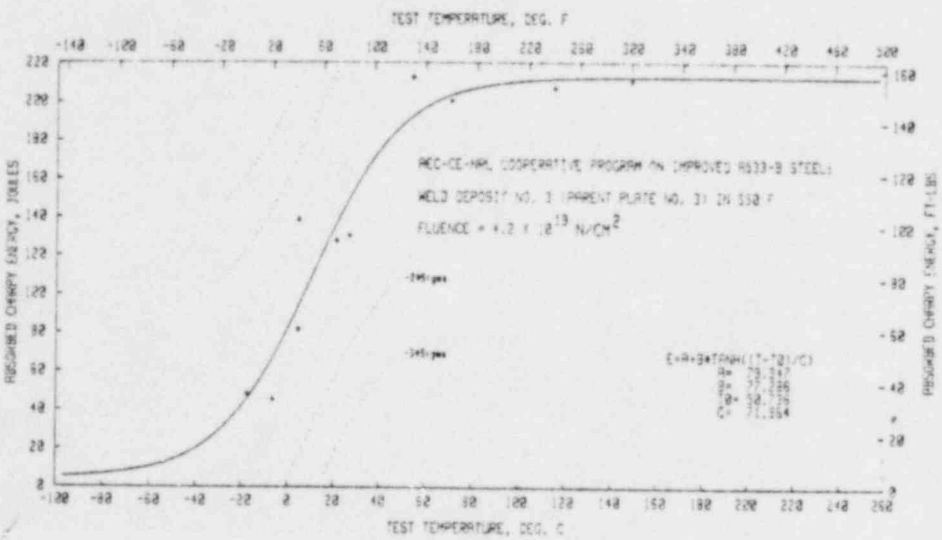
TEST TEMPERATURE, DEG. F
REC-CE-NRL COOPERATIVE PROGRAM ON IMPROVED A533-B STEEL:
WELD DEPOSIT NO. 3 (PARENT PLATE NO. 3) IN 550 F
FLUENCE = 4.2 X 10^19 N/CM^2
E=A+B*TANH((T-T0)/C)
A= 79.547
B= 77.286
T0= 50.726
C= 71.364
ABSORBED CHARPY ENERGY, JOULES
ABSORBED CHARPY ENERGY, FT-LBS.
TEST TEMPERATURE, DEG. C

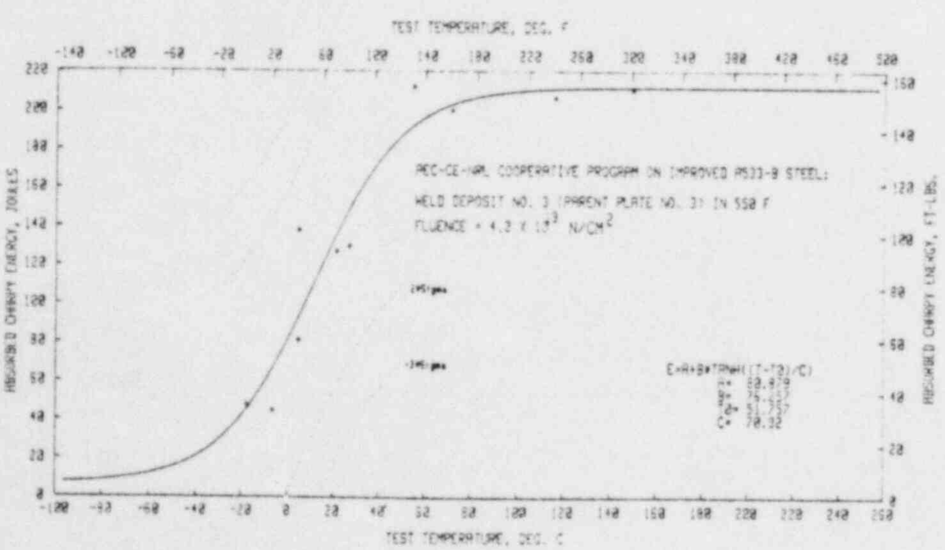
TEST TEMPERATURE, DEG. F
REC-CE-NRL COOPERATIVE PROGRAM ON IMPROVED A533-B STEEL:
WELD DEPOSIT NO. 3 (PARENT PLATE NO. 3) IN 550 F
FLUENCE = 4.2 X 10^3 N/CM^2
E=A+B*TANH((T-T0)/C)
C= 70.32
ABSORBED CHARPY ENERGY, JOULES
ABSORBED CHARPY ENERGY, FT-LBS.
TEST TEMPERATURE, DEG. C

Fig. 4. Absorbed Charpy impact energy vs temperature for irradiated A533B steel with hyperbolic tangent fits for three initial conditions: (a) no added low temperature point, (b) and (c) added point at -232 C, 7 J (-450 F, 5 ft-lb) with numerical weights of 0.1 and 1.0 respectively. This is a very sparse data set (7 points). Positive values of lower shelf energy are obtained only for the fully weighted "fictitious" data point. It is important to note that for all three fits, the 41 and 68 J (30 and 50 ft-lb) test values vary by only 5 Centigrade degrees (10 Fahrenheit degrees).

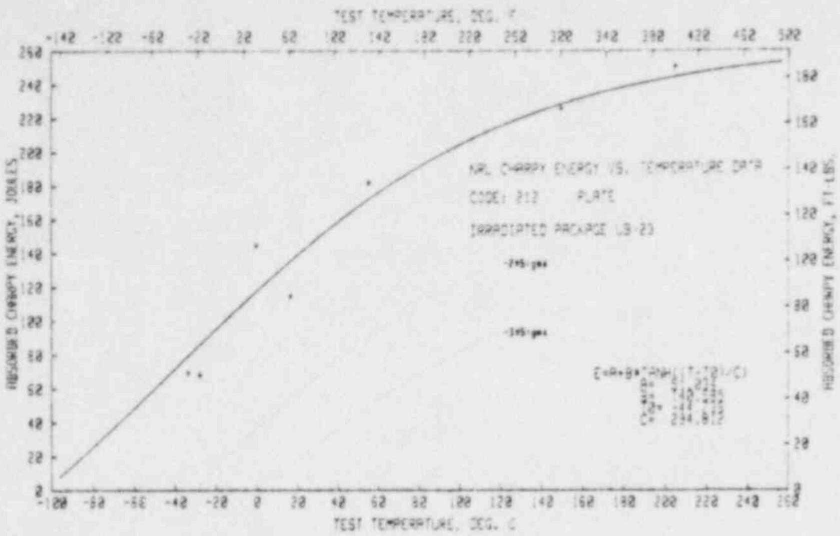
TEST TEMPERATURE, DEG. F
ABSORBED CHARPY ENERGY, JOULES
ABSORBED CHARPY ENERGY, FT-LBS.
NRL CHARPY ENERGY VS. TEMPERATURE DATA
CODE: 212 PLATE
IRRADIATED PACKAGE UB-23
E=A+B*TANH((T-T0)/C)
C= 234.812
TEST TEMPERATURE, DEG. C

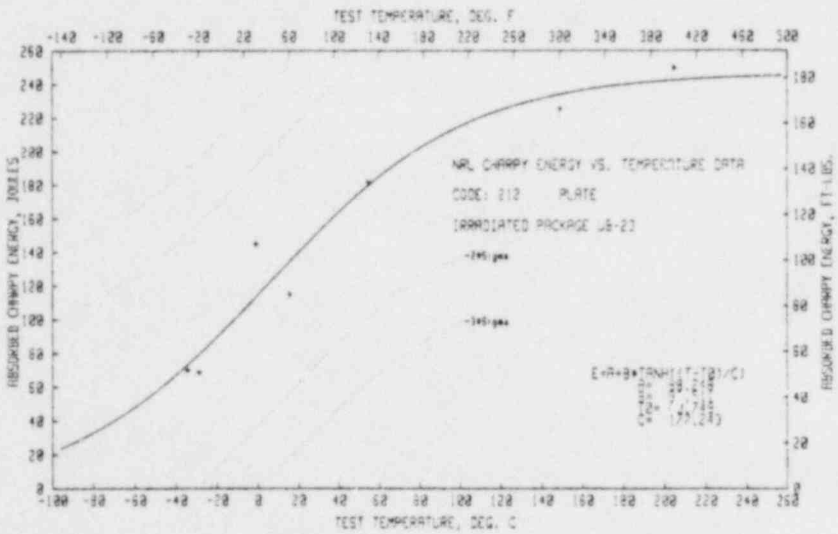
TEST TEMPERATURE, DEG. F
ABSORBED CHARPY ENERGY, JOULES
ABSORBED CHARPY ENERGY, FT-LBS.
NRL CHARPY ENERGY VS. TEMPERATURE DATA
CODE: 212 PLATE
IRRADIATED PACKAGE UB-23
E=A+B*TANH((T-T0)/C)
TEST TEMPERATURE, DEG. C

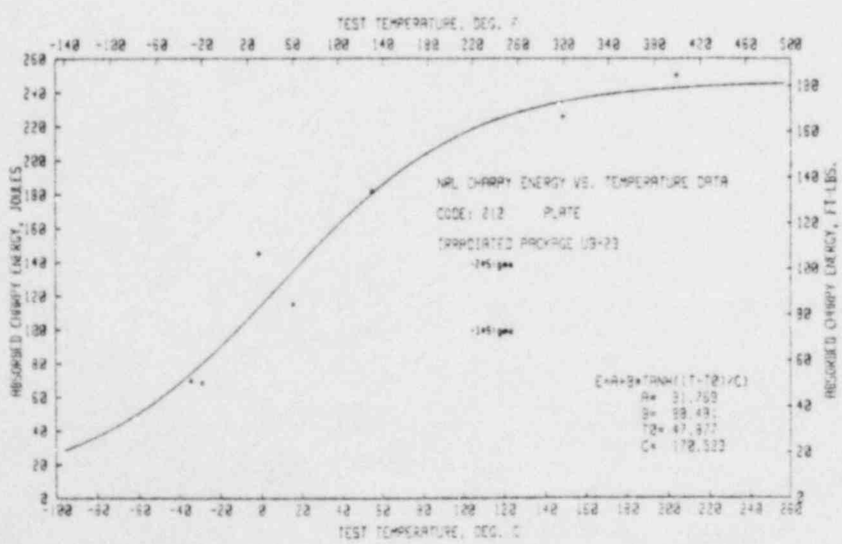
TEST TEMPERATURE, DEG. F
ABSORBED CHARPY ENERGY, JOULES
ABSORBED CHARPY ENERGY, FT-LBS.
NRL CHARPY ENERGY VS. TEMPERATURE DATA
CODE: 212 PLATE
IRRADIATED PACKAGE UB-23
E=A+B*TANH((T-T0)/C)
A= 31.759
B= 98.491
T0= 47.977
C= 170.523
TEST TEMPERATURE, DEG. C

Fig. 5. Absorbed Charpy impact energy vs temperature for unirradiated A533B steel with hyperbolic tangent fits for three initial conditions: (a) no added low temperature point, (b) and (c) added point at -232 C, 7 J (-450 F, 5ft-lb) with numerical weights of 0.1 and 1.0 respectively. These data points are distributed through the transition and onto the upper shelf, but a lower shelf is not defined. In (a) the fit fails according to the positive lower shelf criterion, but (see Table lb) all other criteria seem satisfied and do not vary significantly upon use or incorporation of the additional "fictitious" data point.

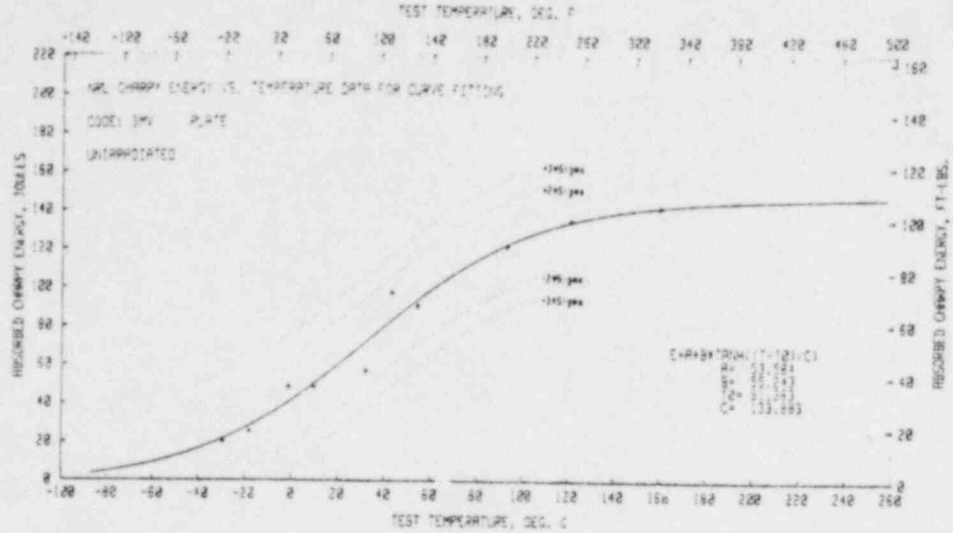

TEST TEMPERATURE, DEG. F
NRL CHARPY ENERGY VS. TEMPERATURE DATA FOR CURVE FITTING
CODE: 3MV PLATE
UNIRRADIATED
ABSORBED CHARPY ENERGY, JOULES
ABSORBED CHARPY ENERGY, FT-LBS.
E=A+B*TANH((T-T0)/C)
TEST TEMPERATURE, DEG. C

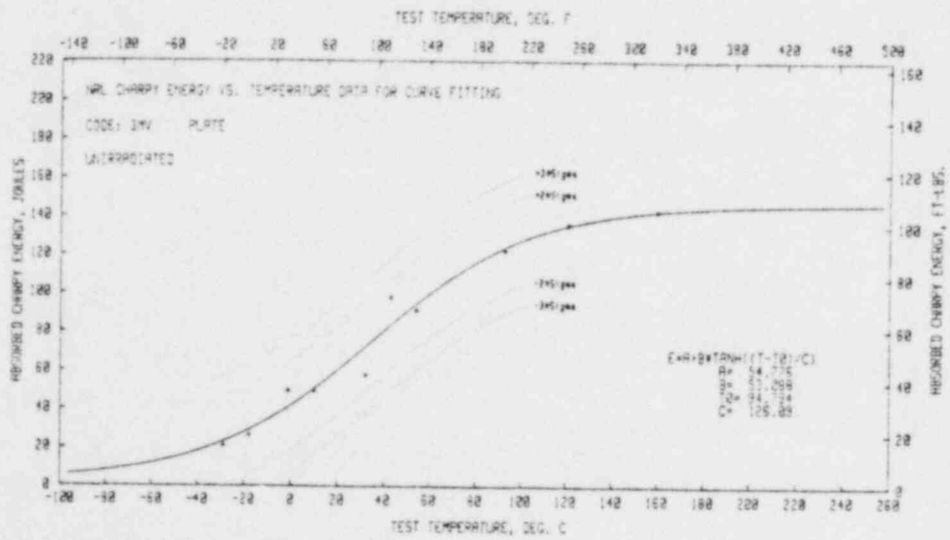

TEST TEMPERATURE, DEG. F
NRL CHARPY ENERGY VS. TEMPERATURE DATA FOR CURVE FITTING
CODE: 3MV PLATE
UNIRRADIATED
ABSORBED CHARPY ENERGY, JOULES
ABSORBED CHARPY ENERGY, FT-LBS.
E=A+B*TANH((T-T0)/C)
A= 54.775
B= 51.298
T0= 94.724
C= 125.89
TEST TEMPERATURE, DEG. C

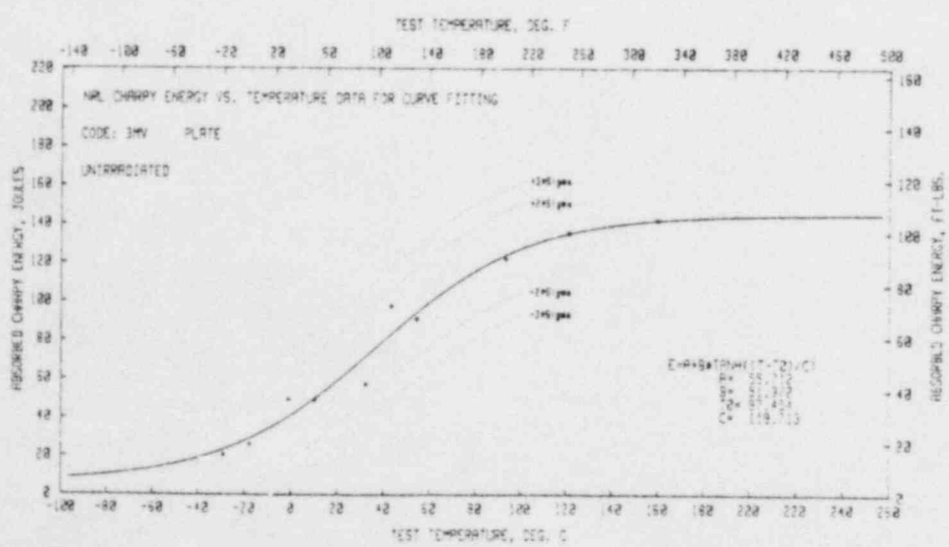

TEST TEMPERATURE, DEG. F
NRL CHARPY ENERGY VS. TEMPERATURE DATA FOR CURVE FITTING
CODE: 3MV PLATE
UNIRRADIATED
ABSORBED CHARPY ENERGY, JOULES
ABSORBED CHARPY ENERGY, FT-LBS.
E=A+B*TANH((T-T0)/C)
TEST TEMPERATURE, DEG. C

Fig. 6. Absorbed Charpy impact energy vs temperature for irradiated weld metal (A533B parent plate) with hyperbolic tangent fits for three initial conditions: (a) no added low temperature point, (b) and (c) added point at -232 C, 7 J (-450 F, 5 ft- lb) with numerical weights of 0.1 and 1.0 respectively. As in Fig. 5, this data set does not extend so as to clearly define a lower shelf. The fit without a "fictitious" data point fails, but incorporation of this additional point results in successful fits with little alteration of key values (See Table Ib).

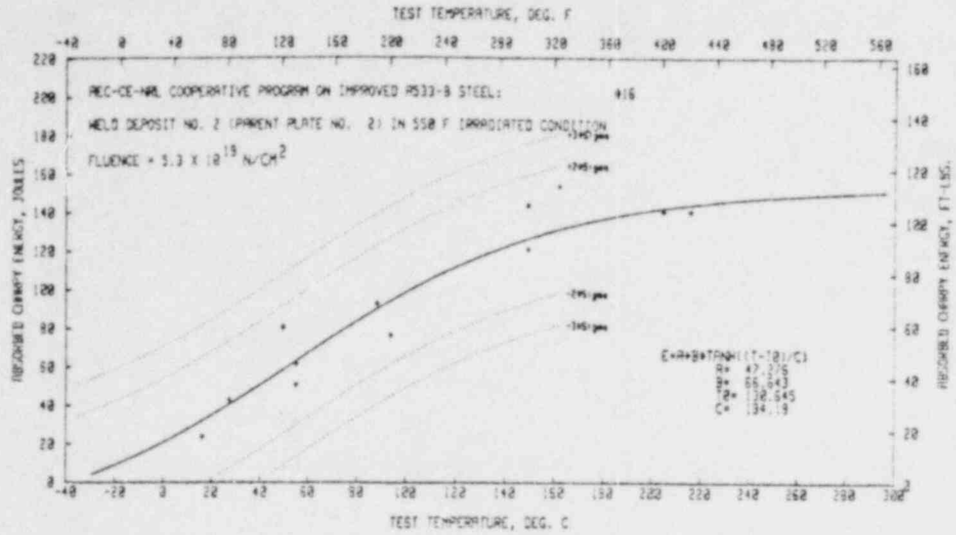
TEST TEMPERATURE, DEG. F
AEC-CE-NRL COOPERATIVE PROGRAM ON IMPROVED A533-B STEEL:
#16
WELD DEPOSIT NO. 2 (PARENT PLATE NO. 2) IN 550 F IRRADIATED CONDITION
FLUENCE = 5.3 X 10^19 N/CM^2
E=A+B*TANH((T-T0)/C)
A= 47.276
B= 66.643
T0= 130.645
C= 134.19
ABSORBED CHARPY ENERGY, JOULES
ABSORBED CHARPY ENERGY, FT-LBS.
TEST TEMPERATURE, DEG. C

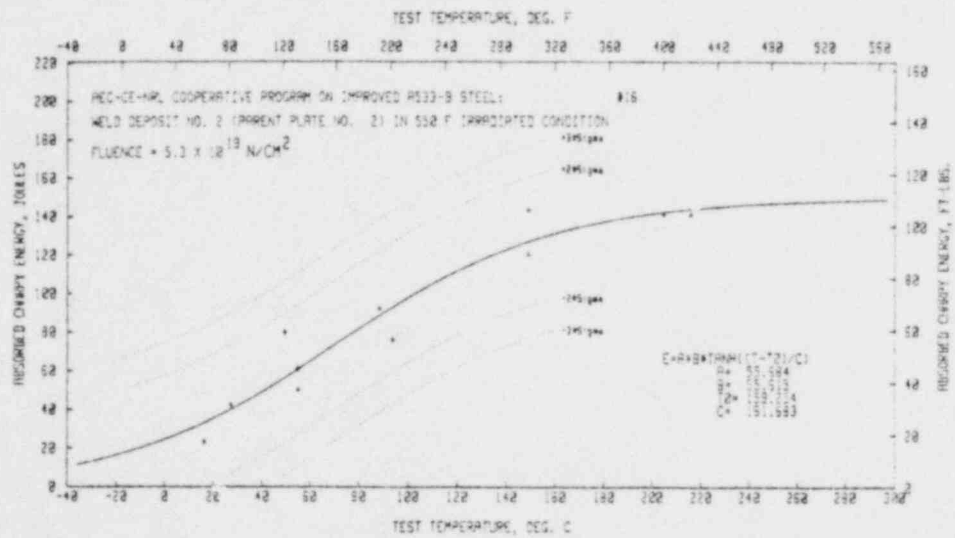
TEST TEMPERATURE, DEG. F
AEC-CE-NRL COOPERATIVE PROGRAM ON IMPROVED A533-B STEEL:
#16
WELD DEPOSIT NO. 2 (PARENT PLATE NO. 2) IN 550 F IRRADIATED CONDITION
FLUENCE = 5.3 X 10^19 N/CM^2
E=A+B*TANH((T-T0)/C)
A= 53.584
C= 151.593
ABSORBED CHARPY ENERGY, JOULES
ABSORBED CHARPY ENERGY, FT-LBS.
TEST TEMPERATURE, DEG. C

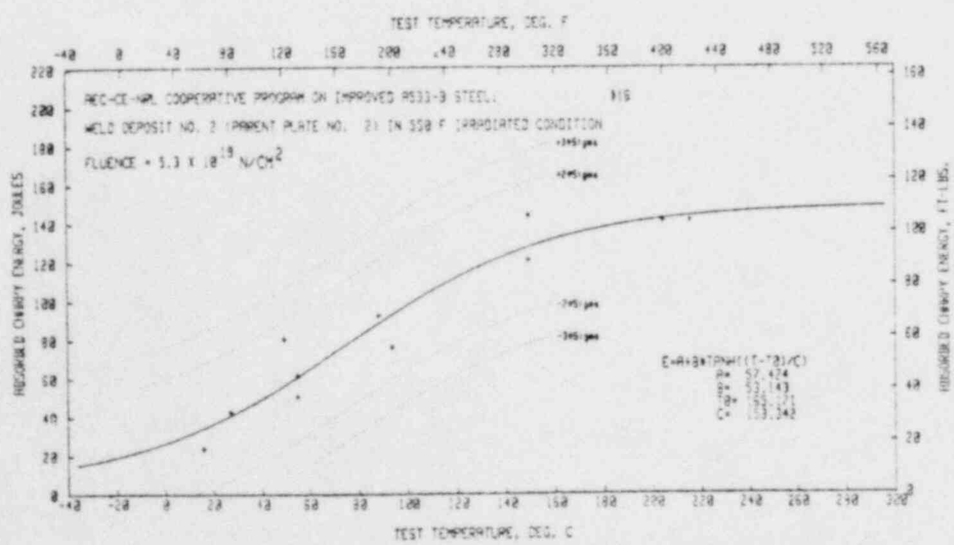
TEST TEMPERATURE, DEG. F
AEC-CE-NRL COOPERATIVE PROGRAM ON IMPROVED A533-B STEEL:
#16
WELD DEPOSIT NO. 2 (PARENT PLATE NO. 2) IN 550 F IRRADIATED CONDITION
FLUENCE = 5.3 X 10^19 N/CM^2
E=A+B*TANH((T-T0)/C)
A= 57.474
B= 53.143
C= 153.242
ABSORBED CHARPY ENERGY, JOULES
ABSORBED CHARPY ENERGY, FT-LBS.
TEST TEMPERATURE, DEG. C

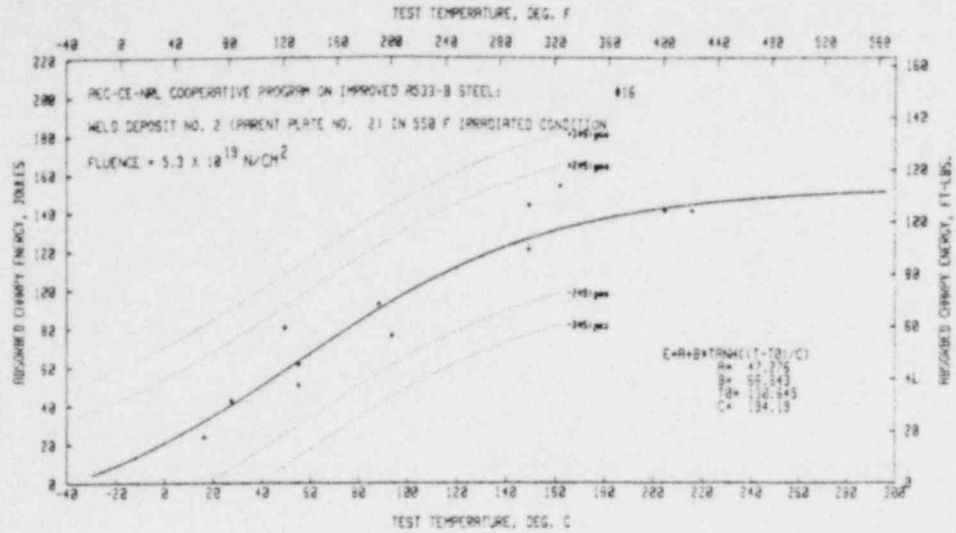
TEST TEMPERATURE, DEG. F
REC-CE-NRL COOPERATIVE PROGRAM ON IMPROVED A533-B STEEL:
#16
WELD DEPOSIT NO. 2 (PARENT PLATE NO. 2) IN 550 F IRRADIATED CONDITION
FLUENCE = 5.3 X 10^19 N/CM^2
ABSORBED CHARPY ENERGY, JOULES
ABSORBED CHARPY ENERGY, FT-LBS.
E=A+B*TANH((T-T0)/C)
C= 134.19
TEST TEMPERATURE, DEG. C

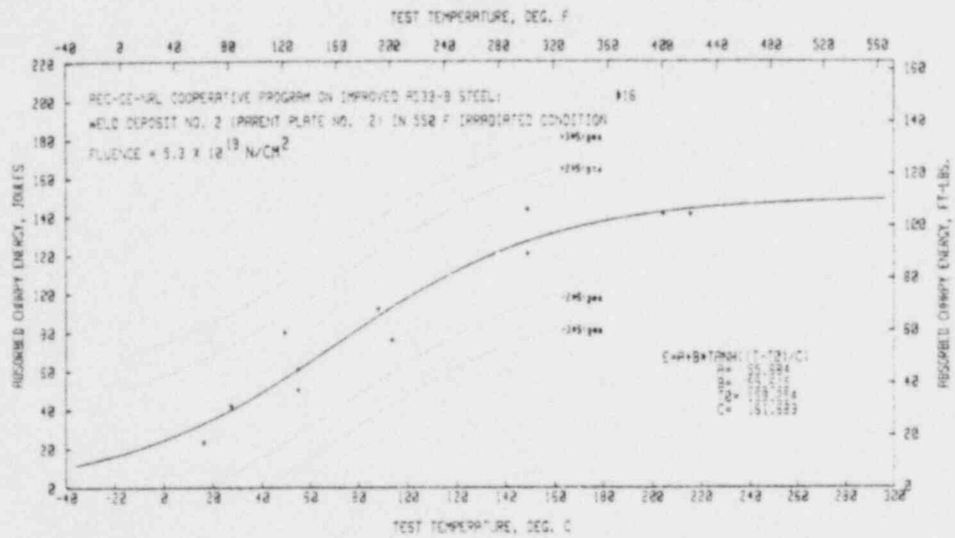
TEST TEMPERATURE, DEG. F
REC-CE-NRL COOPERATIVE PROGRAM ON IMPROVED A533-B STEEL:
#16
WELD DEPOSIT NO. 2 (PARENT PLATE NO. 2) IN 550 F IRRADIATED CONDITION
FLUENCE = 5.3 X 10^19 N/CM^2
ABSORBED CHARPY ENERGY, JOULES
ABSORBED CHARPY ENERGY, FT-LBS.
E=A+B*TANH((T-T0)/C)
TEST TEMPERATURE, DEG. C

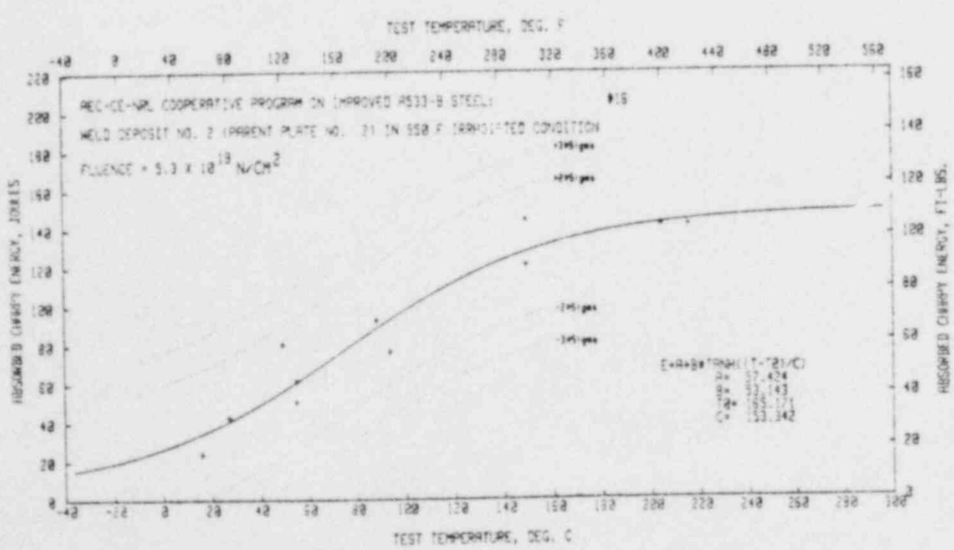
TEST TEMPERATURE, DEG. F
REC-CE-NRL COOPERATIVE PROGRAM ON IMPROVED A533-B STEEL:
#16
WELD DEPOSIT NO. 2 (PARENT PLATE NO. 2) IN 550 F IRRADIATED CONDITION
FLUENCE = 5.3 X 10^19 N/CM^2
ABSORBED CHARPY ENERGY, JOULES
ABSORBED CHARPY ENERGY, FT-LBS.
E=A+B*TANH((T-T0)/C)
A= 57.424
C= 153.342
TEST TEMPERATURE, DEG. C

Fig. 7. Absorbed Charpy impact energy vs temperature for irradiated A533B steel with hyperbolic tangent fits for three initial condtions: (a) no added low temperature point, (b) and (c) added point at -232 C, 7 J (-450 F, 5 ft-lb) with numerical weights of 0.1 and 1.0 respectively. This data set contains a very clearly defined transition region and upper shelf, but no discernible lower shelf. All three fits failed, although the trend toward positive values of the lower shelf energy is clear (See Table lb). Although the transition temperature, as computed by the three fits, shifted by 10 Centigrade degrees (20 Fahrenheit degrees, see Table lb) the 41 and 68 J (30 and 50 ft-lb) temperatures show an insignificant shift.

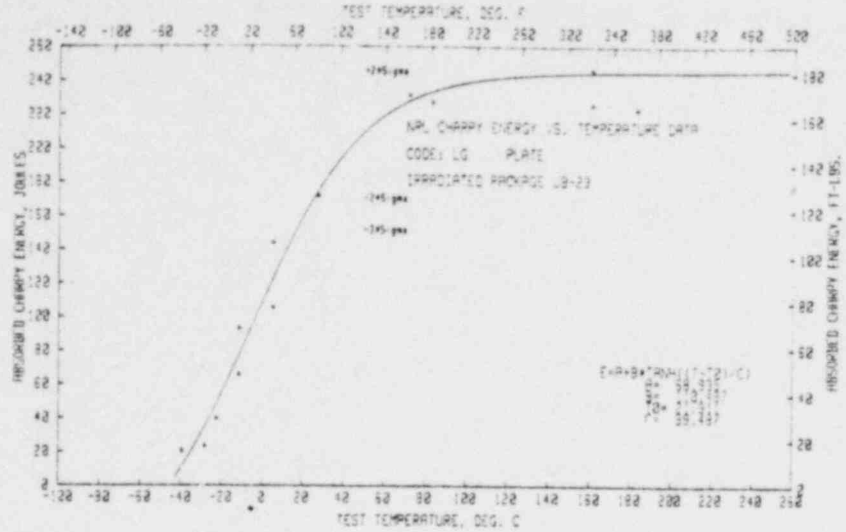
TEST TEMPERATURE, DEG. F
NRL CHARPY ENERGY VS. TEMPERATURE DATA
CODE: LG PLATE
IRRADIATED PACKAGE UB-23
E=A+B*TANH((T-T0)/C)
ABSORBED CHARPY ENERGY, JOULES
ABSORBED CHARPY ENERGY, FT-LBS.
TEST TEMPERATURE, DEG. C

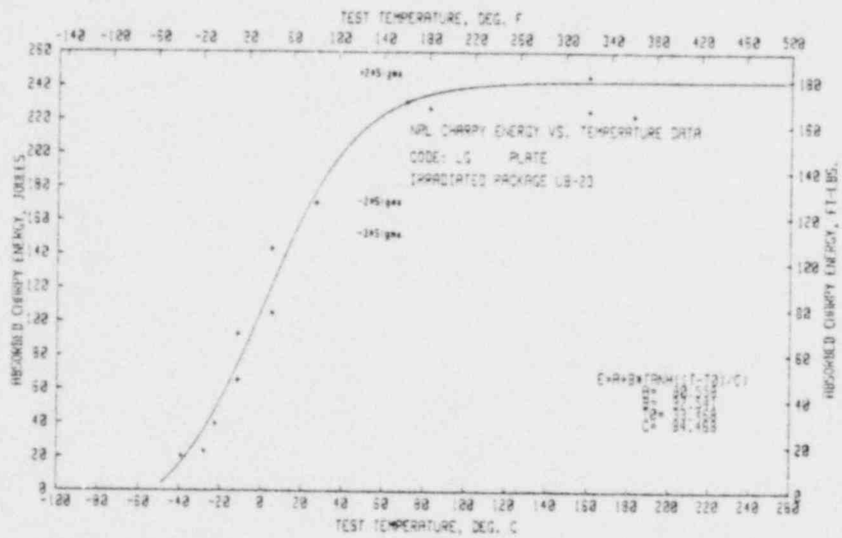
TEST TEMPERATURE, DEG. F
NRL CHARPY ENERGY VS. TEMPERATURE DATA
CODE: LG PLATE
IRRADIATED PACKAGE UB-23
E=A+B*TANH((T-T0)/C)
ABSORBED CHARPY ENERGY, JOULES
ABSORBED CHARPY ENERGY, FT-LBS.
TEST TEMPERATURE, DEG. C

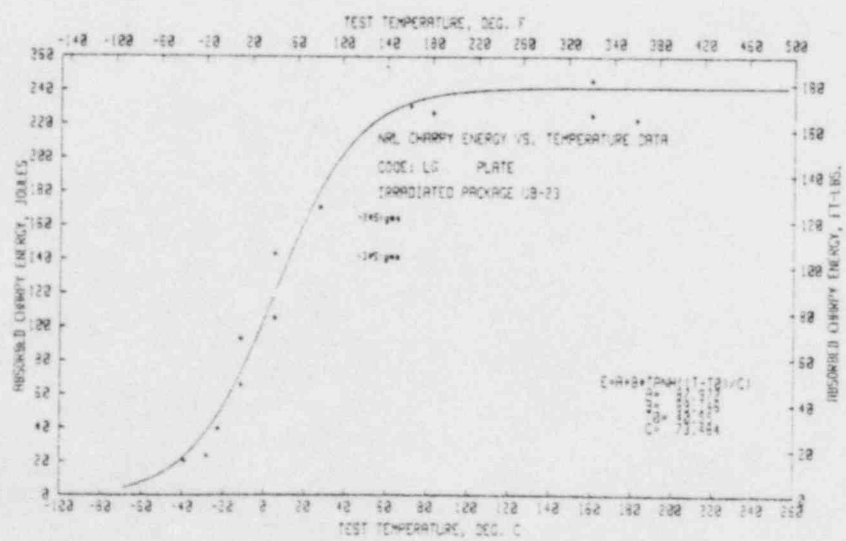
TEST TEMPERATURE, DEG. F
NRL CHARPY ENERGY VS. TEMPERATURE DATA
CODE: LG PLATE
IRRADIATED PACKAGE UB-23
E=A+B*TANH((T-T0)/C)
ABSORBED CHARPY ENERGY, JOULES
ABSORBED CHARPY ENERGY, FT-LBS.
TEST TEMPERATURE, DEG. C

Fig. 8. Absorbed Charpy impact energy vs temperature for heat-affected zone of irradiated A533B steel parent plate with hyperbolic tangents fits for three initial conditions: (a) no added low temperature point, (b) and (c) added point a -232 C, 7 J (-450 F, 5 ft-lb) with numerical weights of 0.1 and 1.0 respectively. This data set exhibits large scatter, no discernible lower or upper shelf, and fits without an added point are not valid. Adding the "fictitious" point creates upper and lower shelf values (Table 1) which cannot be substantiated on the basis of this data set.

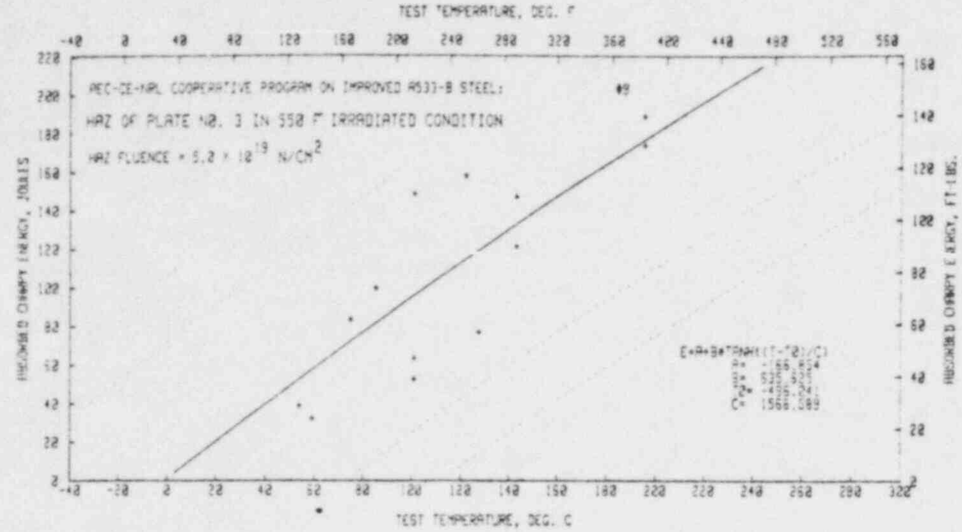
TEST TEMPERATURE, DEG. F
AEC-CE-NRL COOPERATIVE PROGRAM ON IMPROVED A533-B STEEL:
HAZ OF PLATE NO. 3 IN 550 F IRRADIATED CONDITION
HAZ FLUENCE = 5.2 X 10^19 N/CM^2
ABSORBED CHARPY ENERGY, JOULES
ABSORBED CHARPY ENERGY, FT-LBS.
E=A+B*TANH((T-T0)/C)
A= -166.854
B= 535.525
T0= -456.241
C= 1568.089
TEST TEMPERATURE, DEG. C

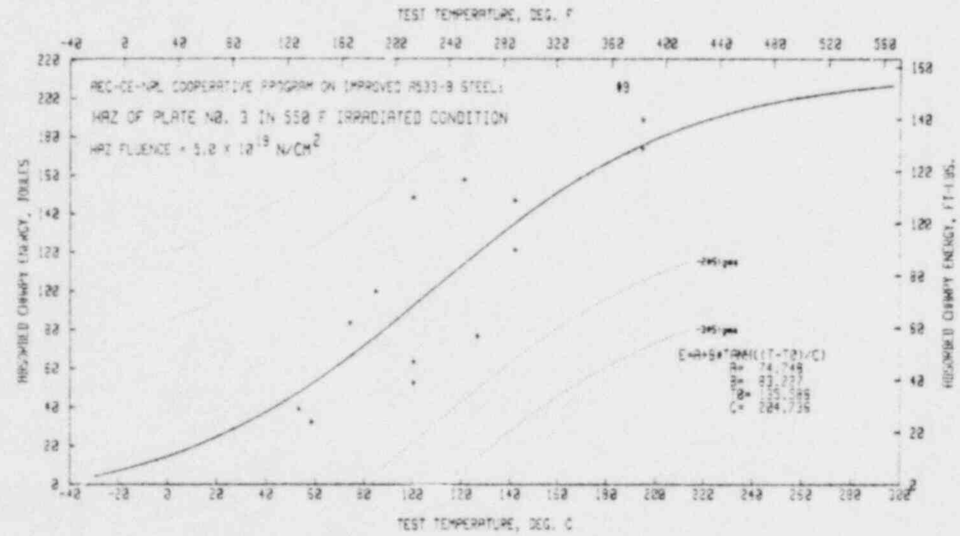
TEST TEMPERATURE, DEG. F
AEC-CE-NRL COOPERATIVE PROGRAM ON IMPROVED A533-B STEEL:
HAZ OF PLATE NO. 3 IN 550 F IRRADIATED CONDITION
HAZ FLUENCE = 5.0 X 10^19 N/CM^2
ABSORBED CHARPY ENERGY, JOULES
ABSORBED CHARPY ENERGY, FT-LBS.
E=A+B*TANH((T-T0)/C)
A= 74.748
B= 83.227
T0= 135.385
C= 204.735
TEST TEMPERATURE, DEG. C

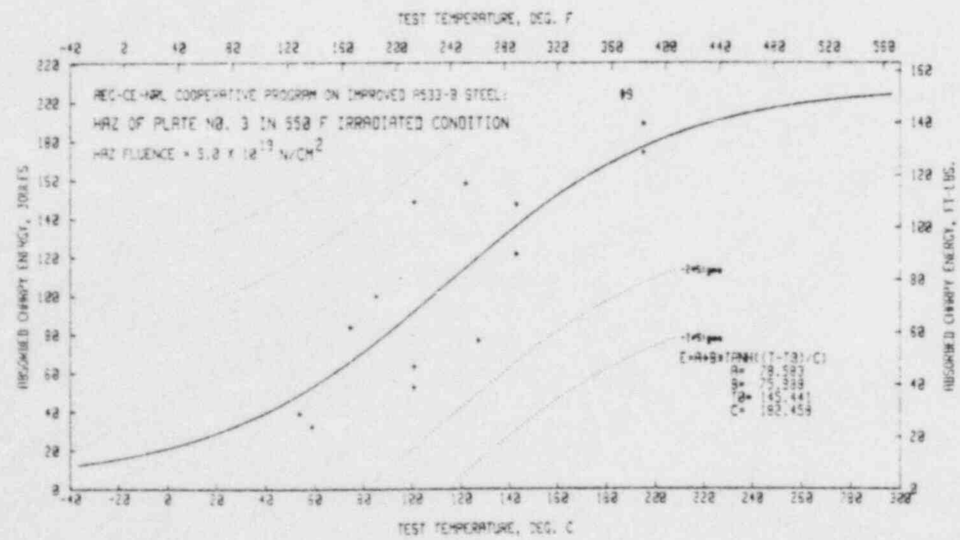
TEST TEMPERATURE, DEG. F
AEC-CE-NRL COOPERATIVE PROGRAM ON IMPROVED A533-B STEEL:
HAZ OF PLATE NO. 3 IN 550 F IRRADIATED CONDITION
HAZ FLUENCE = 5.0 X 10^19 N/CM^2
ABSORBED CHARPY ENERGY, JOULES
ABSORBED CHARPY ENERGY, FT-LBS.
E=A+B*TANH((T-T0)/C)
A= 78.583
B= 75.338
T0= 145.441
C= 192.459
TEST TEMPERATURE, DEG. C

Fig. 9. Absorbed Charpy impact energy vs temperature for irradiated A533B steel, with hyperbolic tangent fits for three initial conditions: (a) no added low temperature point, (b) and (c) added point at -232 C, 7 J (-450 F, 5 ft-lb) with numerical weights of 0.1 and 1.0 respectively. This data set, which might be better described with a two-stage, or "double hump" curve, cannot be so described by the hyperbolic tangent in its present form.

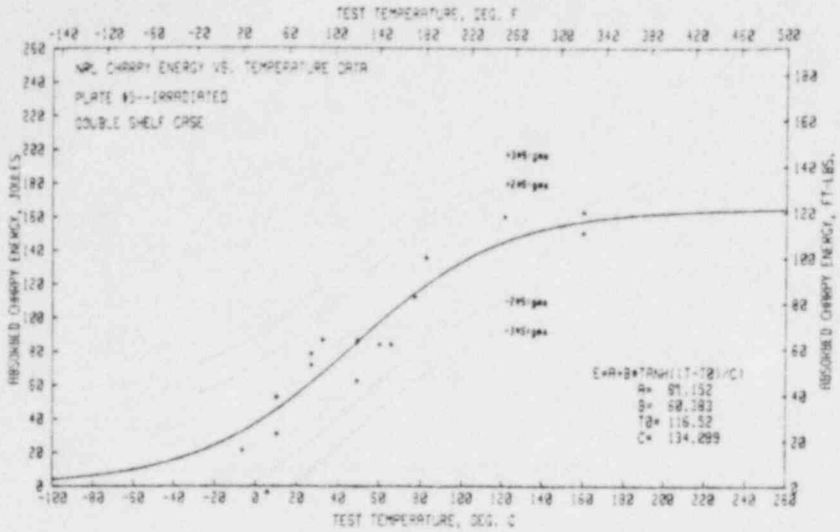
TEST TEMPERATURE, DEG. F
NRL CHARPY ENERGY VS. TEMPERATURE DATA
PLATE #5--IRRADIATED
DOUBLE SHELF CASE
E=A+B*TANH((T-T0)/C)
A= 61.152
B= 60.383
T0= 116.52
C= 134.299
ABSORBED CHARPY ENERGY, JOULES
ABSORBED CHARPY ENERGY, FT-LBS.
TEST TEMPERATURE, DEG. C

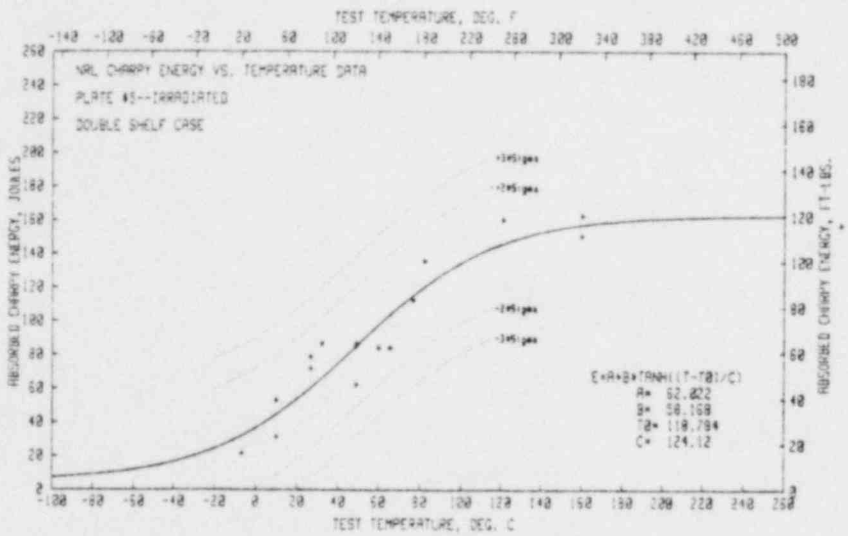
TEST TEMPERATURE, DEG. F
NRL CHARPY ENERGY VS. TEMPERATURE DATA
PLATE #5--IRRADIATED
DOUBLE SHELF CASE
E=A+B*TANH((T-T0)/C)
A= 62.022
B= 58.168
T0= 118.794
C= 124.12
ABSORBED CHARPY ENERGY, JOULES
ABSORBED CHARPY ENERGY, FT-LBS.
TEST TEMPERATURE, DEG. C

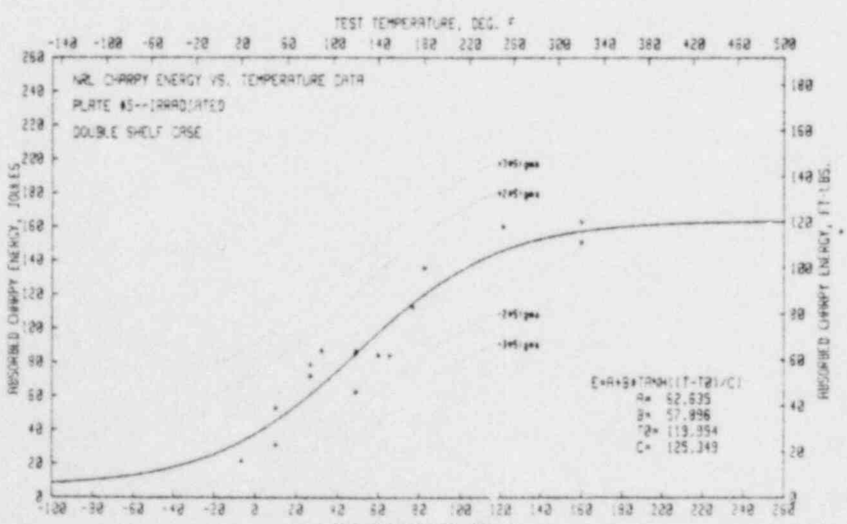
TEST TEMPERATURE, DEG. F
NRL CHARPY ENERGY VS. TEMPERATURE DATA
PLATE #5--IRRADIATED
DOUBLE SHELF CASE
E=A+B*TANH((T-T0)/C)
A= 62.635
B= 57.896
T0= 119.354
C= 125.349
ABSORBED CHARPY ENERGY, JOULES
ABSORBED CHARPY ENERGY, FT-LBS.
TEST TEMPERATURE, DEG. C

Fig. 10. The upper shelf continues to rise somewhat in this very well-defined data set. The agreement between the computed and estimated values is excellent, however.

Fig. 11. This data set (ASTM A302-B Reference Plate) is included as an example of what happens when the upper shelf is not well defined, i.e. tests do not extend beyond first indication of 100% shear fracture temperature. The illustration shows that the computed value of the upper shelf could be very misleading. Note, however, the agreement between the 41 and 68 J values as computed and estimated by the authors.

The panel shown in Fig. 12 represents the computational results for a data set which have been singled out for special discussion. In all curve fitting procedures, involving data with a significant amount of scatter, the user is often uncertain as to whether the algorithm has successfully converged to the one set of coefficients producing a true minimization of the residuals, or whether the computations have converged on a set of values which represent a local minimization. Whether or not the true minima is attained is most often dependent on the choice of initial guesses made by the user. An example of this difficulty is illustrated by Fig. 12. This shows hyperbolic tangent curves using two sets of guessed coefficients, and the curves using the final coefficients computer—determined for each set. It is unfortunate that the "best" fit, is the one which does not produce a 41 joule temperature value. There is no "sure-fire" way to avoid this sort of dilemma. It is a mathematical and common-sense fact that the more data points and the lower the standard deviation, the more likely is the convergence to a single minima.

CONCLUSIONS

The consideration of these results leads to the following conclusions:

(a) For the most part, the computed models produce results which agree well with one another.

(b) When the data sets are complete, that is, they exhibit an essentially sigmoidal shape, the agreement between the computed results and authors' estimates is quite good.

(c) As a refinement of (a) and (b) above the transition region parameters, that is, the 41 and 68 J level temperatures are in quite good agreement, with the authors estimates always equal to or conservatively positioned with respect to the computed results. Where the data clearly defines an upper shelf region, that value too is in good agreement with the hyperbolic tangent model.

(d) The effect of forcing the hyperbolic tangent model to furnish a positive value of the lower shelf energy has little detrimental effect on those cases which would do that even without such a constraint, and has a very beneficial effect on those data sets which need such help. In spite of this constraint, the data sets of Figs 8 and 11 still failed to generate plausible values of the upper shelf energy. Accordingly curve fitting procedure applied during testing can guide but should not dictate the selection of test temperatures in surveillance programs.

This page is left intentionally blank

Fig. 10. Absorbed Charpy impact energy vs temperature for irradiated weld metal, with hyperbolic tangent fits for three initial conditions: (a) no added low temperature point, (b) and (c) added point at -232 C, 7 J (-450 F, 5 ft-lb) with numerical weights of 0.1 and 1.0 respectively. In spite of the rising upper shelf, the large number of data points in the transition region results in an accurate fit within the transition at the slight expense of an accurate upper shelf value. The lower shelf value is somewhat influenced by the "fictitious" data point.

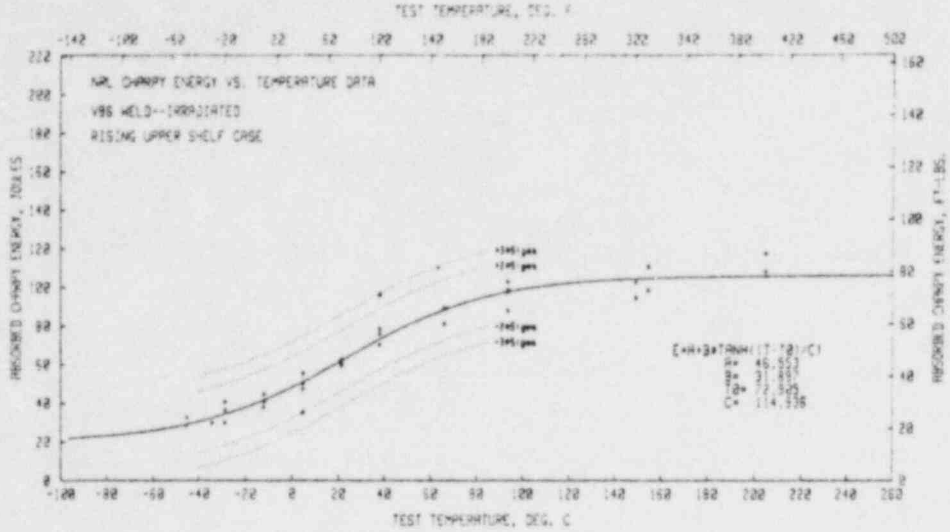
TEST TEMPERATURE, DEG. F
NRL CHARPY ENERGY VS. TEMPERATURE DATA
V86 WELD--IRRADIATED
RISING UPPER SHELF CASE
ABSORBED CHARPY ENERGY, JOULES
ABSORBED CHARPY ENERGY, FT-LBS.
E=A+B*TANH((T-T0)/C)
A= 46.553
T0= 72.325
C= 114.536
TEST TEMPERATURE, DEG. C

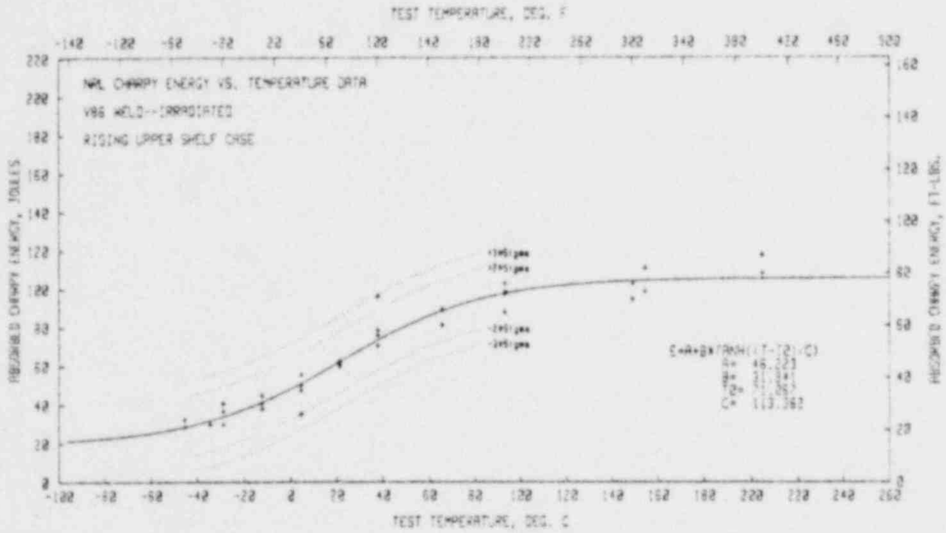
TEST TEMPERATURE, DEG. F
NRL CHARPY ENERGY VS. TEMPERATURE DATA
V86 WELD--IRRADIATED
RISING UPPER SHELF CASE
ABSORBED CHARPY ENERGY, JOULES
ABSORBED CHARPY ENERGY, FT-LBS.
E=A+B*TANH((T-T0)/C)
A= 46.223
C= 113.362
TEST TEMPERATURE, DEG. C

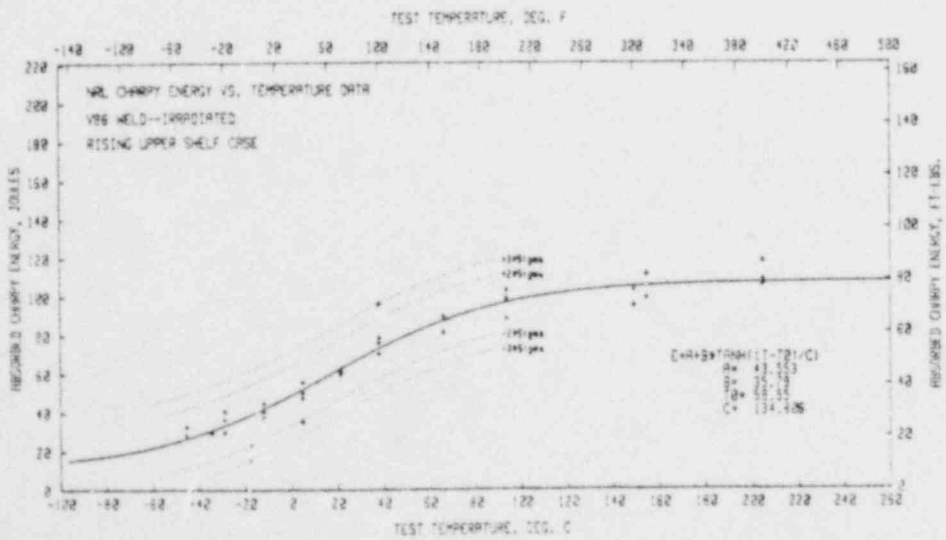
TEST TEMPERATURE, DEG. F
NRL CHARPY ENERGY VS. TEMPERATURE DATA
V86 WELD--IRRADIATED
RISING UPPER SHELF CASE
ABSORBED CHARPY ENERGY, JOULES
ABSORBED CHARPY ENERGY, FT-LBS.
E=A+B*TANH((T-T0)/C)
A= 43.553
TEST TEMPERATURE, DEG. C

Fig. 11. Absorbed Charpy impact energy vs temperature for A302B steel, with hyperbolic tangent fits for three initial conditions: (a) no added low temperature point, (b) and (c) added point at -232 C, 7 J (-450 F, 5 ft-lb) with numerical weights of 0.1 and 1.0 respectively. This data set, with no discernible upper shelf defined by the data, generates an unusual, but mathematically accurate fit to the data. Obviously, the low-temperature data point has little effect on the definition of the upper shelf, and all three fits produce absurd computations of the upper shelf energy.

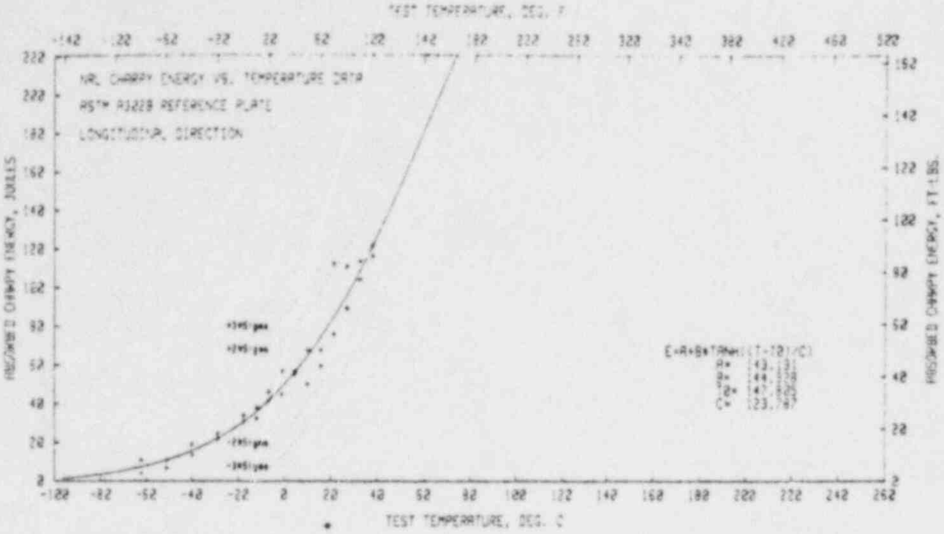
TEST TEMPERATURE, DEG. F
NRL CHARPY ENERGY VS. TEMPERATURE DATA
ASTM A302B REFERENCE PLATE
LONGITUDINAL DIRECTION
ABSORBED CHARPY ENERGY, JOULES
ABSORBED CHARPY ENERGY, FT-LBS.
+3*Sigma
+2*Sigma
-2*Sigma
-3*Sigma
E=A+B*TANH((T-T0)/C)
TEST TEMPERATURE, DEG. C

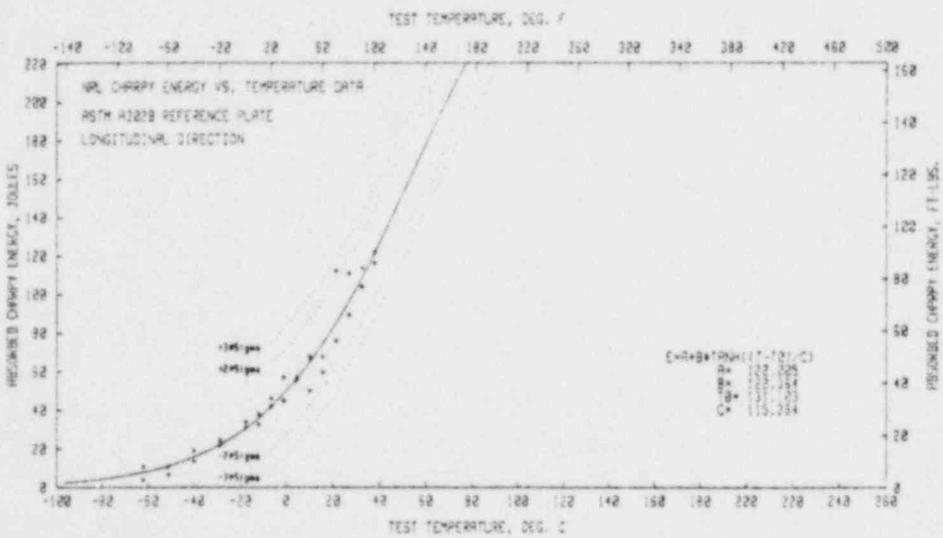
TEST TEMPERATURE, DEG. F
NRL CHARPY ENERGY VS. TEMPERATURE DATA
ASTM A302B REFERENCE PLATE
LONGITUDINAL DIRECTION
ABSORBED CHARPY ENERGY, JOULES
ABSORBED CHARPY ENERGY, FT-LBS.
+3*Sigma
+2*Sigma
-2*Sigma
-3*Sigma
E=A+B*TANH((T-T0)/C)
C= 115.394
TEST TEMPERATURE, DEG. C

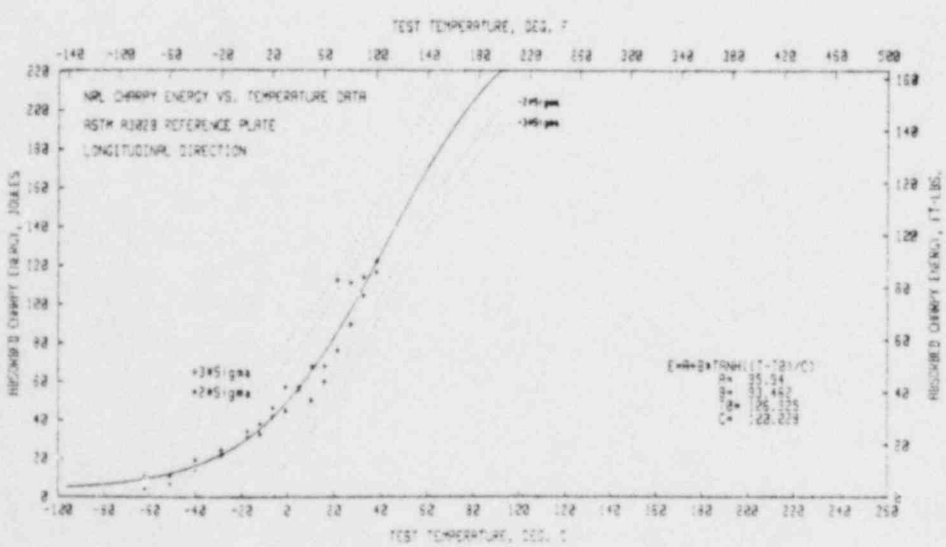
TEST TEMPERATURE, DEG. F
NRL CHARPY ENERGY VS. TEMPERATURE DATA
ASTM A302B REFERENCE PLATE
LONGITUDINAL DIRECTION
ABSORBED CHARPY ENERGY, JOULES
ABSORBED CHARPY ENERGY, FT-LBS.
-2*Sigma
-3*Sigma
+3*Sigma
+2*Sigma
E=A+B*TANH((T-T0)/C)
A= 35.54
TEST TEMPERATURE, DEG. C

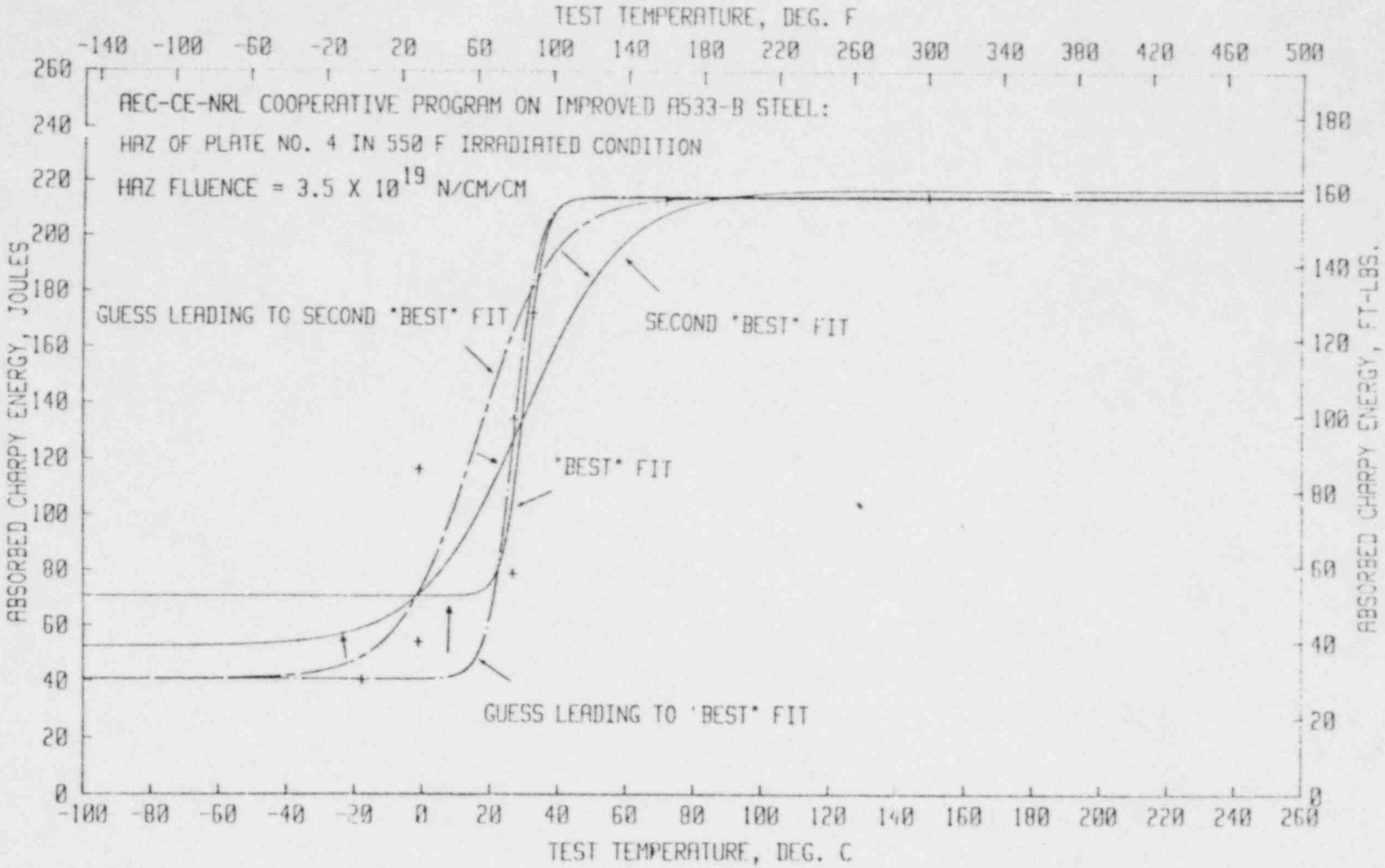
TEST TEMPERATURE, DEG. F
-140 -100 -60 -20 20 60 100 140 180 220 260 300 340 380 420 460 500
AEC-CE-NRL COOPERATIVE PROGRAM ON IMPROVED A533-B STEEL:
HAZ OF PLATE NO. 4 IN 550 F IRRADIATED CONDITION
HAZ FLUENCE = 3.5 X 10^19 N/CM/CM
GUESS LEADING TO SECOND "BEST" FIT
SECOND "BEST" FIT
"BEST" FIT
GUESS LEADING TO "BEST" FIT
ABSORBED CHARPY ENERGY, JOULES
0 20 40 60 80 100 120 140 160 180 200 220 240 260
ABSORBED CHARPY ENERGY, FT-LBS.
0 20 40 60 80 100 120 140 160 180
-100 -80 -60 -40 -20 0 20 40 60 80 100 120 140 160 180 200 220 240 260
TEST TEMPERATURE, DEG. C

Fig. 12 Example of the algorithm settling into a false minima and determining a set of coefficients which are not representative of the "best" fit for the given data. A different initial guess leads to even further minimization of the residuals. Such problems are usually associated with sparse data sets with large scatter, and require very careful, considerate programming to insure that such problems do not arise.

(e) In the cases for which the authors' estimates are influenced by consideration of unirradiated condition data and the expected behavior for the particular material, knowledge which is obviously not available to the computer, there may be substantial differences betweeen computed and estimated values of the important parameters.

ACKNOWLEDGEMENT

This study was sponsored by the U. S. Nuclear Regulatory Commission (NRC). Operating Reactors Division, Materials Engineering Branch.

REFERENCES:

1. J. R. Hawthorne, J. J. Koziol and S. T. Byrne, "Evaluation of Commercial Production A533-B Steel Plates and Weld Deposits with Extra-Low Copper Content for Radiation Resistance." NRL Report 8136, October 1977.

2. J. R. Hawthorne, Editor, the NRC-EPRI Research Program (12P886-2), Evaluation and Prediction of Neutron Embrittlement in Reactor Pressure Vessel Materials, Annual Progress Report for CY 1978, NRL Report 8327, August 30, 1979.

3. F. J. Loss, Editor, Structural Integrity of Water Reactor Pressure Boundary Components, Quarterly Progress Report, April-June 1979, NRL Memorandum Report 4064, NUREG/CR 0943 September 28, 1979.

4. J. R. Hawthorne, Radiation Effects Information Generated on the ASTM Reference Correlation-Monitor Steels, ASTM Data Series 54, 1974.

5. W. Oldfield, "Curve-Fitting Impact Test Data: A Statistical Procedure" ASTM Standardization News 3 (11) November, 1975.

6. W. Oldfield, "Fitting Curves to Toughness Data" ASTM J. Testing and Evaluation, V (6), November, 1979.

7. G. Hofer, C. C. Hung, U. Guenes, "A Mathematical Function for the Description of Charpy Impact Tests, Zeitschsift fur Werkstofftecnik 8 p. 109-111, 1977.